New ICFs for Non-spherical PNe

Denise R. Gonçalves

Observatório do Valongo
Universidade Federal do Rio de Janeiro – UFRJ, Brazil

R. Wesson (ESO); C. Morisset (UNAM); M. Barlow (UCL); B. Ercolano (Muenchen Univ.)

Outline:

- Why PN abundances?
- Deriving PN abundances
- The problem of PN shapes *vs* ICFs
- Our PN 3D photo models *vs* ICFs
- Results: optical + IR spectra

  UV + optical + IR spectra

Why PN abundances?

PNe

- **PNe** are useful probes of ISM composition
- **PNe** provide information about stellar nucleosynthesis of 1 to 8 M⊙ stars
- **PNe** archive progenitor abundances of α-elements
- Abundances derived from PNe reflect the ISM at the time that the progenitor star formed

A few reviews:

- Kwitter & Henry (2012)
  PNe abundances in the Galaxy + MCs
- Magrini, Stanghellini & Gonçalves (2012)
  LG PNe (H II regions) beyond the MCs
- Stasinska 2002 (IAC Winter School 2002)
  PN + H II region abundances

HII regions

Outline:

- Why PN abundances?
- Deriving PN abundances
- The problem of PN shapes *vs* ICFs
- Our PN 3D photo models *vs* ICFs
- Results: optical + IR spectra

  UV + optical + IR spectra

Deriving PN abundances

Mainly two methods

1) *DIRECT (EMPIRICAL)*

Given the limited $\triangle\lambda$, only few lines of some ions can be measured:

➡ unseen ions must be corrected for: ***ICF* method**

– Despite the many problems, ICF for empirical abundance is frequently the only option available

– The higher the λ coverage the better the abundance determination: UV and IR, instead of only optical data, improve enormously the results

– The most common ICFs: Kingsburgh & Barlow (1994; KB94)

Deriving PN abundances

Mainly two methods

1) *DIRECT (EMPIRICAL)*

Given the limited $\triangle\lambda$, only few lines of some ions can be measured:

➨ unseen ions must be corrected for: ***ICF* method**

– Despite the many problems, ICF for empirical abundance is frequently the only option available

– The higher the λ coverage the better the abundance determination: UV and IR, instead of only optical data, improve enormously the results

– The most common ICFs: Kingsburgh & Barlow (1994; KB94)

Based on 1D photoionization models

Deriving PN abundances

Mainly two methods

2) Empirical (*ICF)* abundances are the input abundances for a **Photoionization model fitting**
– the empirical abundances are varied until the predicted line ratios (and emission line maps) match the observations

- Stasinska (2002) has shown that with a too limited number of constraints acceptable photo models can give two families of solutions
- No solution is found – cases on which given the constraints of the gas distribution and ionizing star(s) (Peña et al. 1998; Luridiana et al. 1999; Stasinska & Schaerer 1999)
- Tremendously time consuming

Outline:

- Why PN abundances?
- Deriving PN abundances
- The problem of PN shapes *vs* ICFs
- Our PN 3D photo models *vs* ICFs
- Results: optical + IR spectra

  UV + optical + IR spectra

The problem of PN shapes *vs* ICFs

– There is a strong correlation between macro-morphology and the N abundance (in the Galaxy; Corradi & Schwarz (1995) and also in the MCs (Shaw 2012)

Considering that KB94 recipes are based on 1D (spherical) modelling

and also

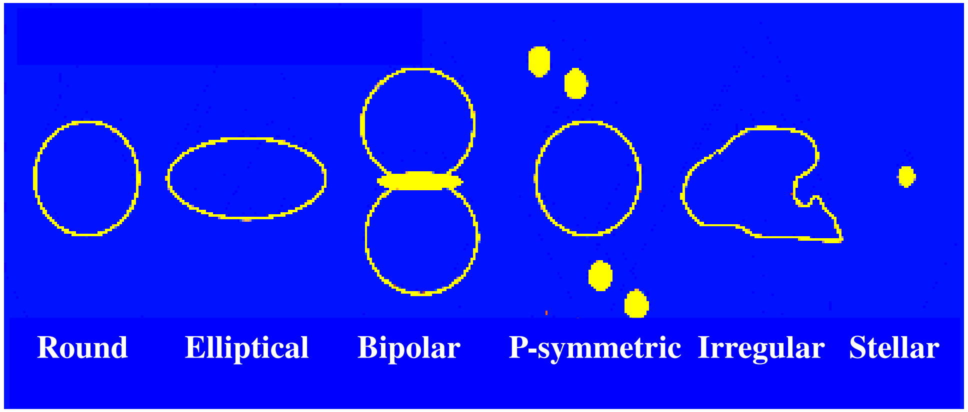

MASH, IPHAS, etc: **~20% of the PNe are round**

Parker (2012)

The problem of PN shapes *vs* ICFs

– There is a strong correlation between macro-morphology and the N abundance (in the Galaxy; Corradi & Schwarz (1995) and also in the MCs (Shaw 2012).

Considering that KB94 recipes are based on 1D (spherical) modelling

and also

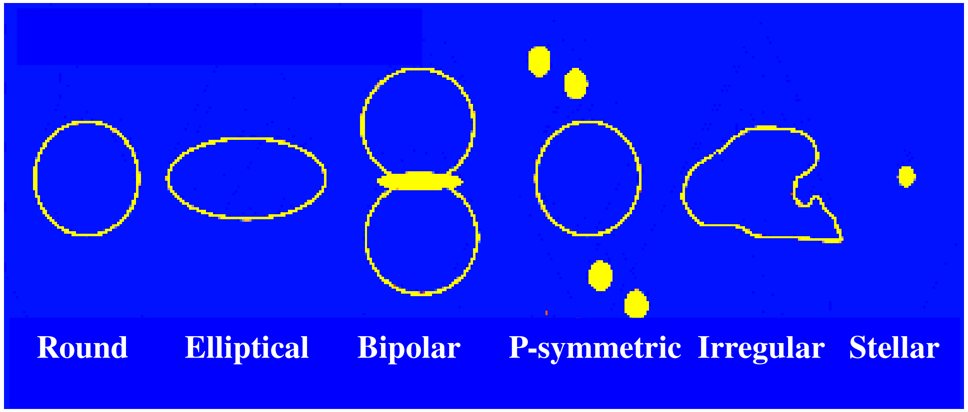

MASH, IPHAS, etc: ~20% of the PNe are round

Parker (2012)

The effect of the shape on the PN abundances –or, how the recipes to determine abundances change with shape– should be explored!

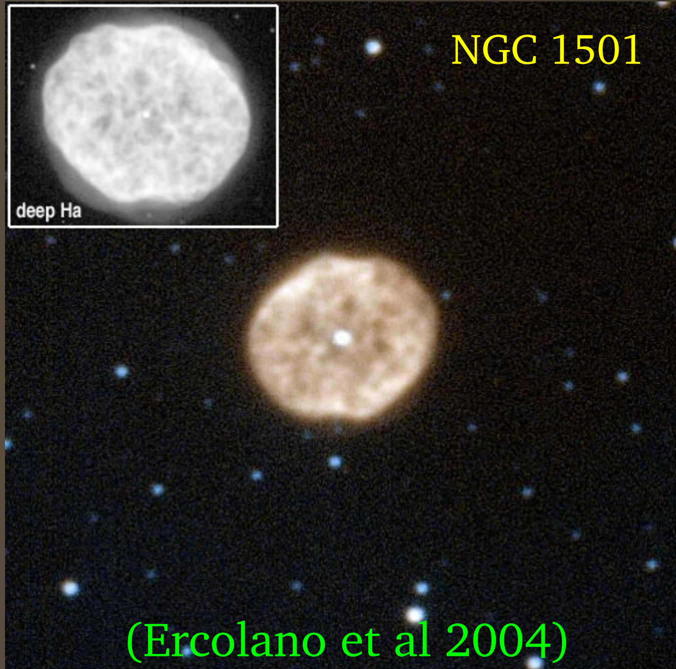

NGC 1501 G144.5+06.5 04:07.0 +60:55:00, R:G:B=log(Ha+[NII]), both, log[OIII]
"The IAC morphological catalog of northern galactic planetary nebulae"
A. Manchado, M.A. Guerrero, L. Stanghellini, M. Serra-Ricart, 1996, ed. IAC
inset: Jay Gallagher (U. Wisconsin)/WIYN/NOAO/NSF, www.noao.edu/image_gallery/html/im0034.html

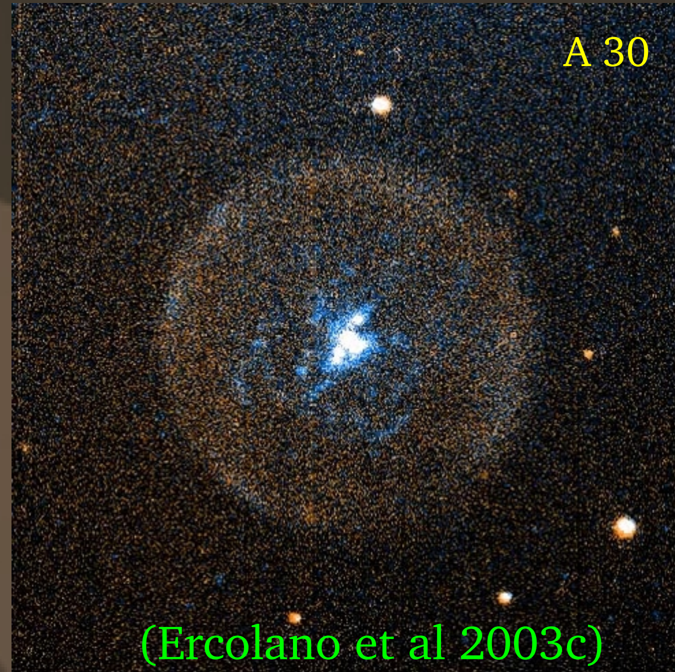

A 30 G208.5+33.2 08:46:54.4 +17:52:33, R:G:B=log(Ha+[NII]), both, log[OIII]
"The IAC morphological catalog of northern galactic planetary nebulae"
A. Manchado, M.A. Guerrero, L. Stanghellini, M. Serra-Ricart, 1996, ed. IAC

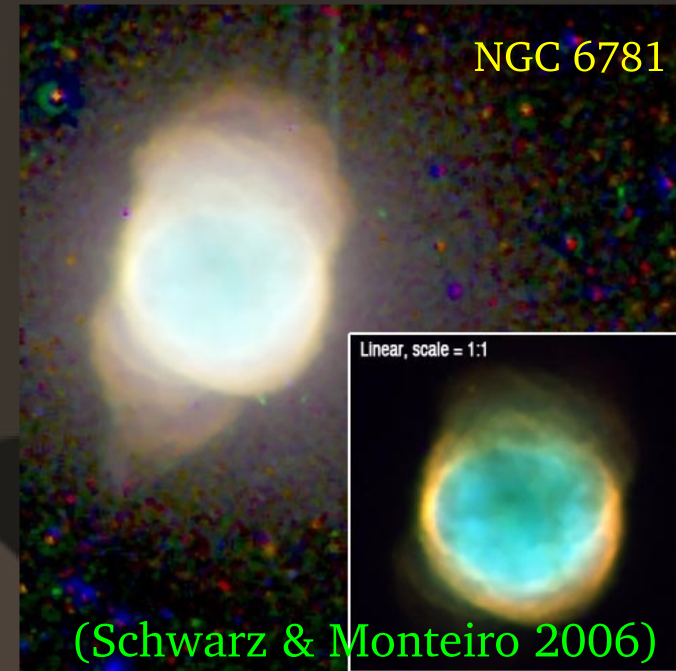

NGC 6781 G041.8-02.9 19 18 28.09 +06 32 19.3 R:G:B = log[NII], log(Ha), log[OIII]
ref: Mavromatakis, F., Papamastorakis, J., Paleologou, E.V., 2001, A&A 374, 280
source: http://www.ing.iac.es/~rcorradi/HALOES/

Mz 1 G322.4-02.6 15 34 17.00 -59 09 09.0, R:G:B=log(Ha+[NII]), both, log[OIII]
ref: Schwarz, H.E., Corradi, R.L.M., Melnick, J 1992 A&A Suppl, 96, 23
image files courtesy R Corradi. N is NOT up. See ref for orientation.

NGC 3132 G272.1+12.3 10 07 01.76 -40 26 11.1 R:G:B=log(Ha+[NII]),both,log[OIII]
ref: Schwarz, H.E., Corradi, R.L.M., Melnick, J 1992 A&A Suppl, 96, 23
image files courtesy R Corradi. N is NOT up. See ref for orientation.

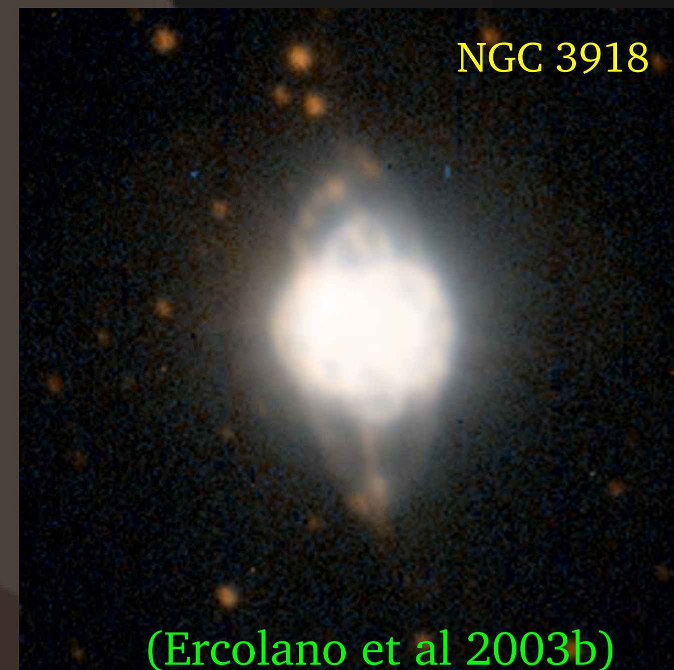

NGC 3918 G294.6+04.7 11 50 17.73 -57 10 56.9, R:G:B=log(Ha+[NII]),both,log[OIII]
ref: Schwarz, H.E., Corradi, R.L.M., Melnick, J 1992 A&A Suppl, 96, 23
image files courtesy R Corradi. N is NOT up. See ref for orientation.

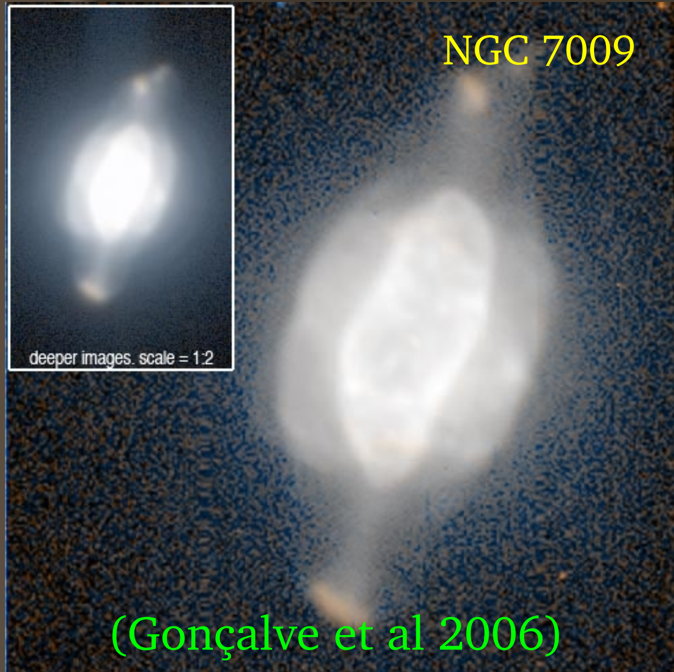

NGC 7009 G037.7-34.5 21 04 10.88 -11 21 48.2, R:G:B=log(Ha+[NII]),both,log[OIII]
ref: Schwarz, H.E., Corradi, R.L.M., Melnick, J 1992 A&A Suppl, 96, 23
image files courtesy R Corradi. N is NOT up. See ref for orientation.

NGC 6369 G002.4+05.8 17 29 20.44 -23 45 34.2, R:G:B=log(Ha+[NII]),both,log[OIII]
ref: Schwarz, H.E., Corradi, R.L.M., Melnick, J 1992 A&A Suppl, 96, 23
image files courtesy R Corradi. N is NOT up. See ref for orientation.

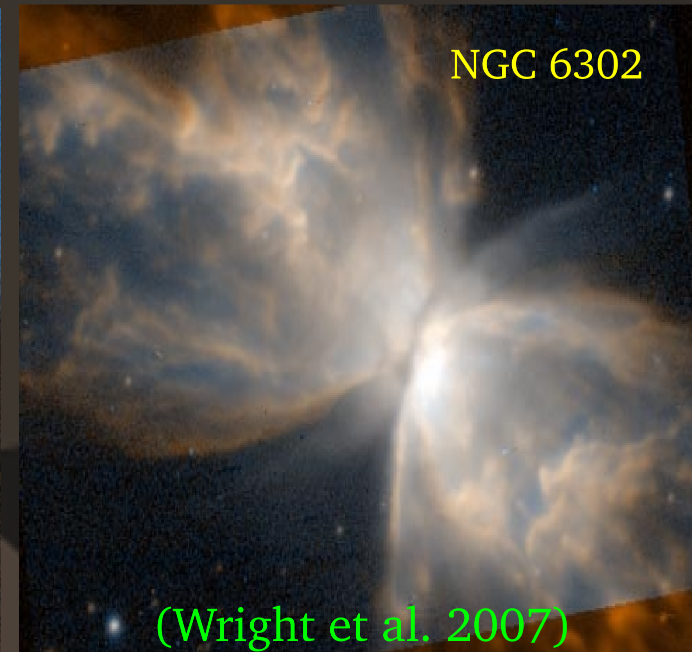

NGC 6302 G349.5+01.0 17 13 44.21 -37 06 15.9 R:G:B=log(Ha+[NII]),both,log[OIII]
ref: Schwarz, H.E., Corradi, R.L.M., Melnick, J 1992 A&A Suppl, 96, 23
image files courtesy R Corradi. N is NOT up. See ref for orientation.

→ By the time of the APNV, we believed that the ionization structures obtained from all these models would allow us to derive the A*ICFs*

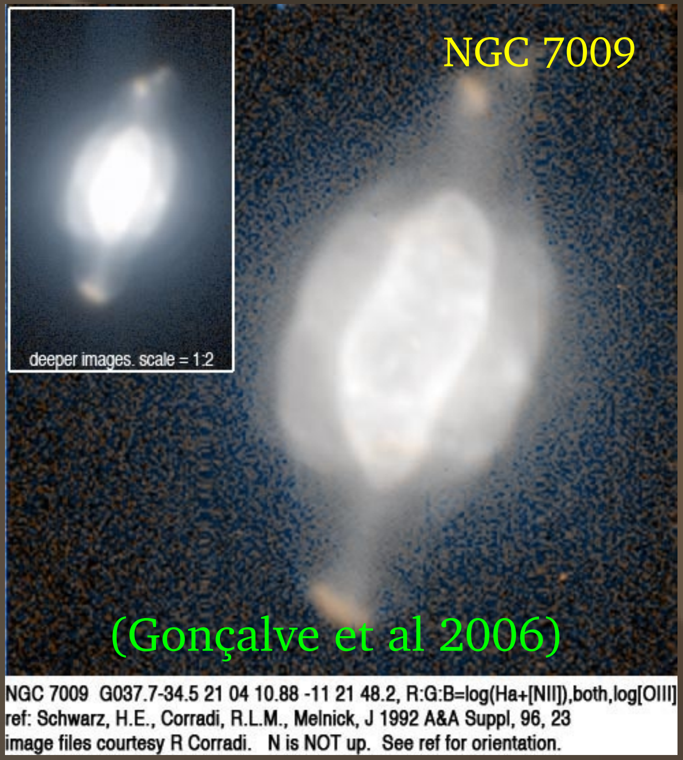

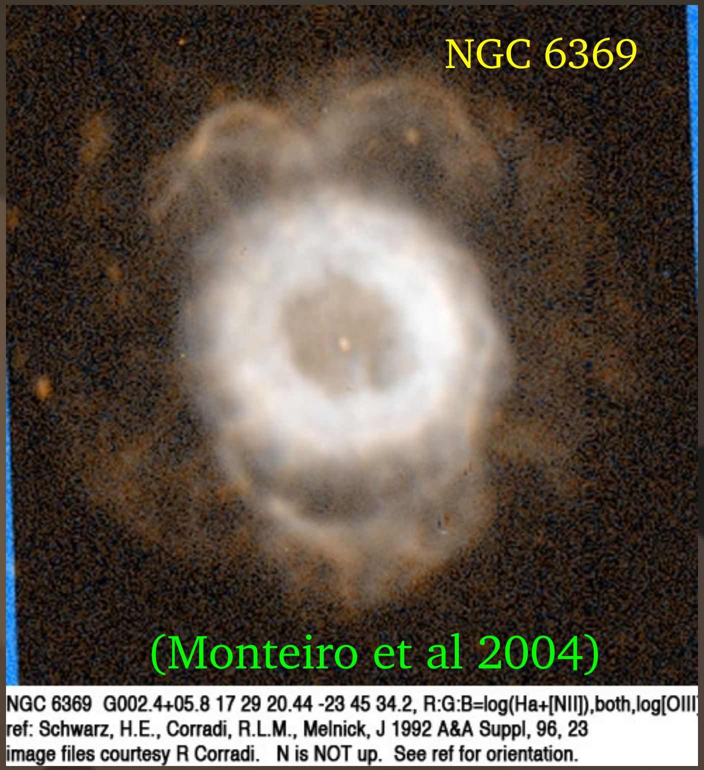

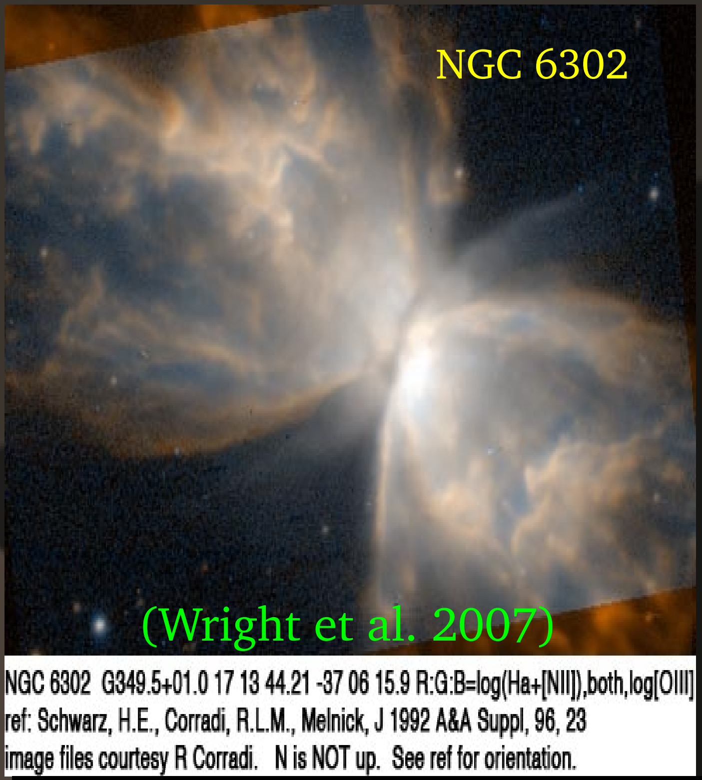

Even though ONE more bipolar PN is being modelled in a 3D fashion (poster A8)

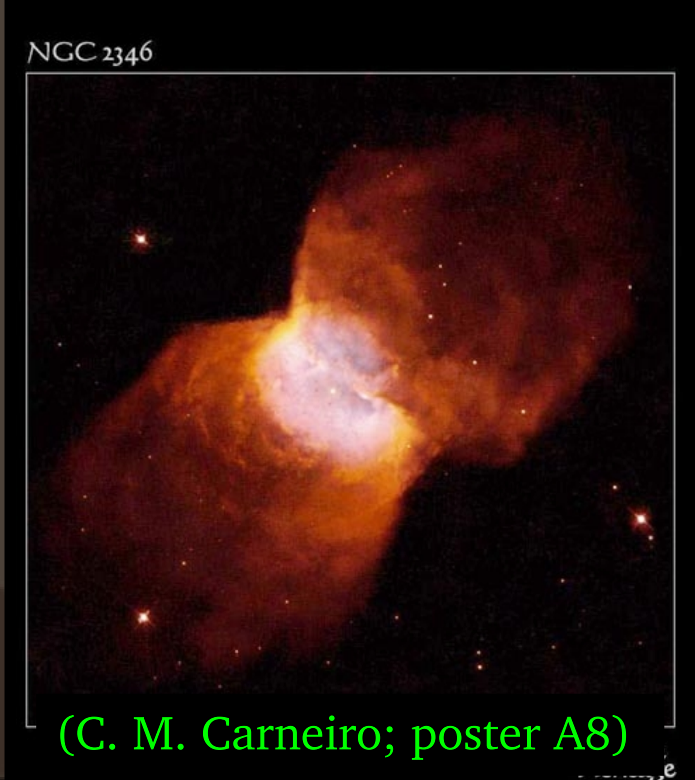

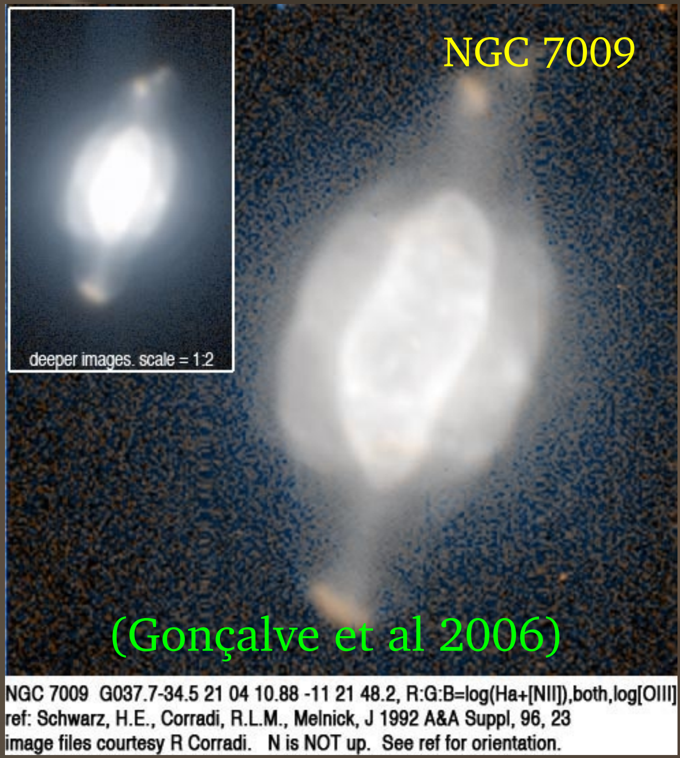

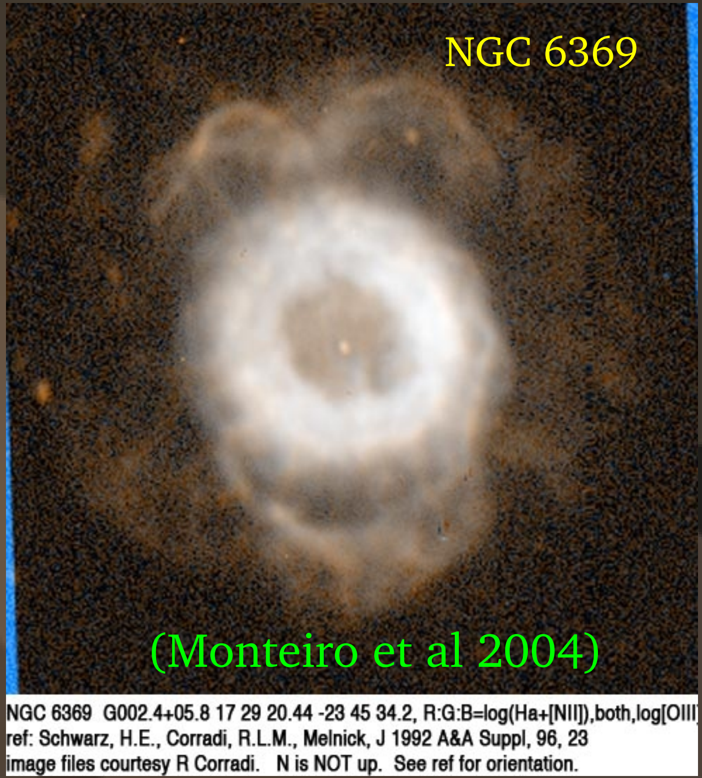

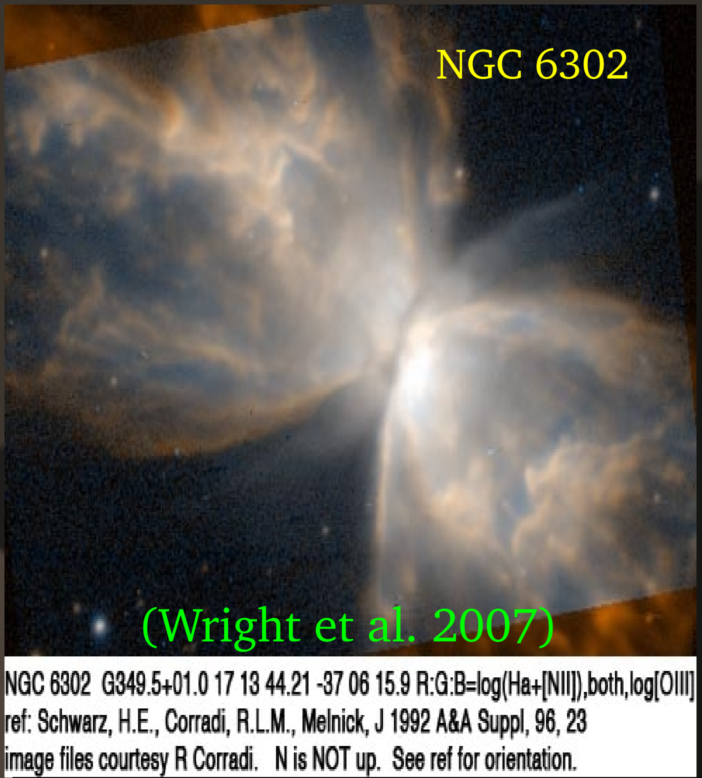

Even though ONE more bipolar PN is being modelled in a 3D fashion (poster A8)

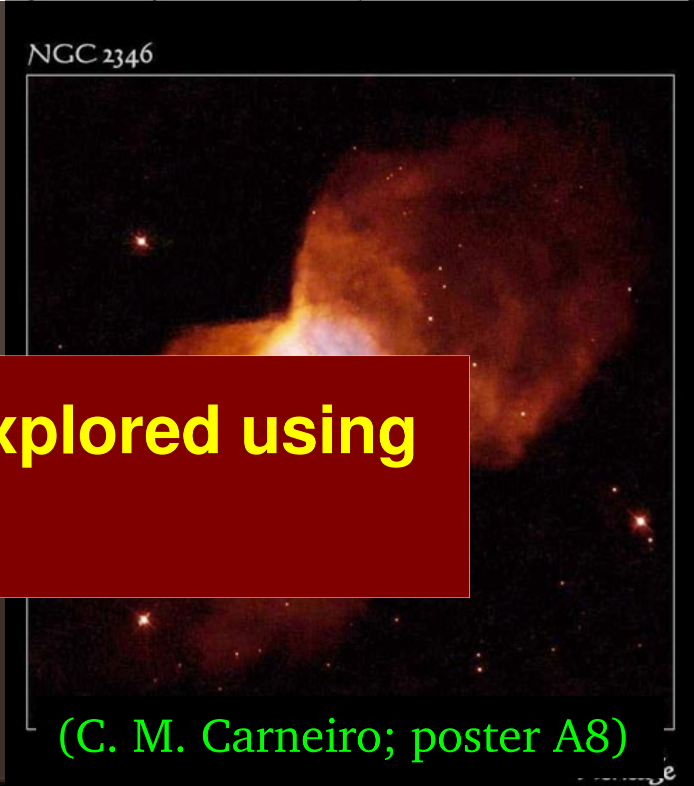

The space of parameters is under explored using the existing 3D PN models!

Outline:

- Why PN abundances?
- Deriving PN abundances
- The problem of PN shapes *vs* ICFs
- Our PN 3D photo models *vs* ICFs
- Results: optical + IR spectra

  UV + optical + IR spectra

Our PN 3D photo models *vs* ICFs

Alexander & Balick (1997)
Gruenwald & Viegas (1998)
Morisset & Stasinska (2008)

MOCASSIN (Ercolano et al. 2003, 05, 08)

Range of Stellar/Nebular Parameters

ContShape: blackbody
$50 \leq T_{eff} \leq 250$ kK
$1.x10^3 \leq L_* \leq 2.x10^4 L_\odot$
X/H: Type I and non-Type I
Geometry: round -R, spherical -E
bipolar - B
Ne: 3 000 cm^{-3}
Size: depends on morphology
(radiation-bounded)

Tafoya et al (2009)

Bipolars have dense torus; 5 – 10 x denser than the lobes

– $Ne_{(torus)} = 6 \times Ne_{(lobes)}$

Our PN 3D photo models *vs* ICFs

Pottasch & Bernard-Salas et al. series of papers

– These authors determined abundances using UV + optical + IR ionic species

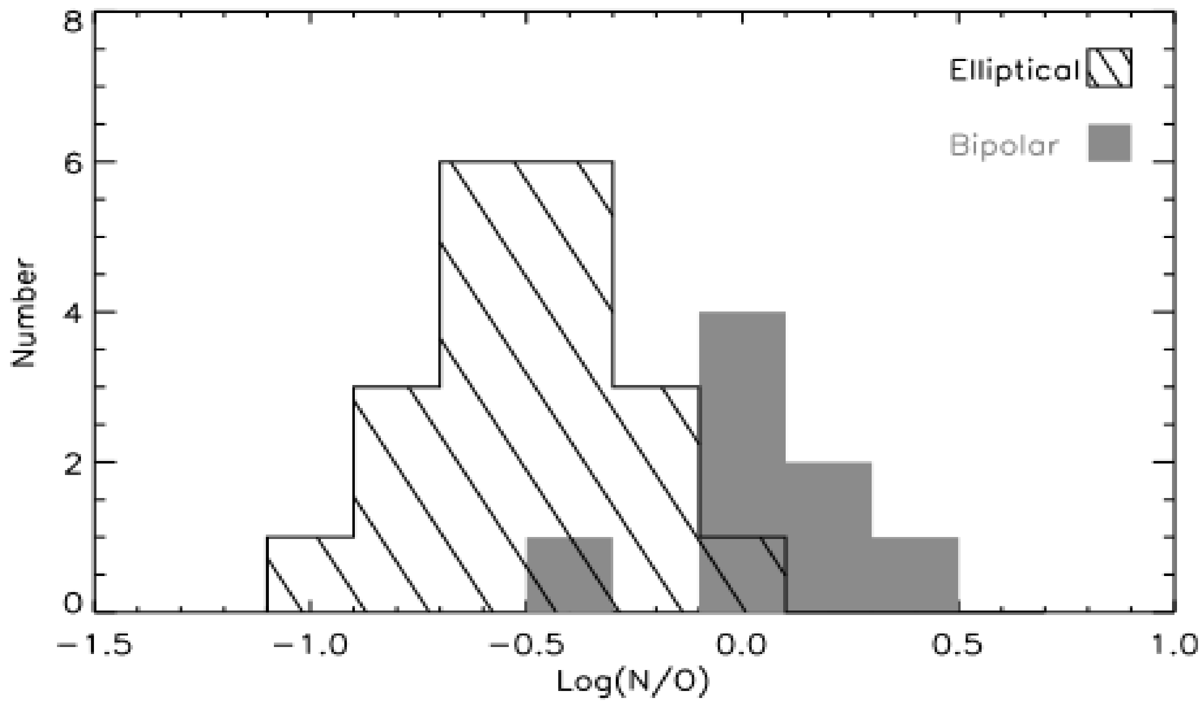

Fig. 1. Histogram of the nitrogen/oxygen ratio of the PNe listed in Table 1. Round PNe are not included in this plot because of the small number of objects.

Altogether they have about 40 PNe with accurately determined abundances

We can test our results against their sample

(Pottasch & Bernard-Salas 2010; Pottasch et al. 2011)

Outline:

- Why PN abundances?
- Deriving PN abundances
- The problem of PN shapes *vs* ICFs
- Our PN 3D photo models *vs* ICFs
- Results: optical + IR spectra

  UV + optical + IR spectra

ICFs for optical (only) data

No matter which is the shape considered, since NO ICFs are needed for He/H we discuss only O, N, Ne, S, Ar

- Only ELLIPTICAL vs BIPOLAR results
- Only in terms of the comparison between the *true* and the *ICF* abundances

ICFs for optical (only) data

No matter which is the shape considered, since NO ICFs are needed for He/H we discuss only O, N, Ne, S, Ar

Not even in the spherical symmetric case the ICFs would recover the "true" (or photo model) total abundances!!!

So ICFs should be revisited also in the case of **ROUND** PNe (Delgado-Inglada; poster A14)

- Only ELLIPTICAL vs BIPOLAR results
- Only in terms of the comparison between the *true* and the *ICF* abundances

Results: the ionization structure changes with shape...

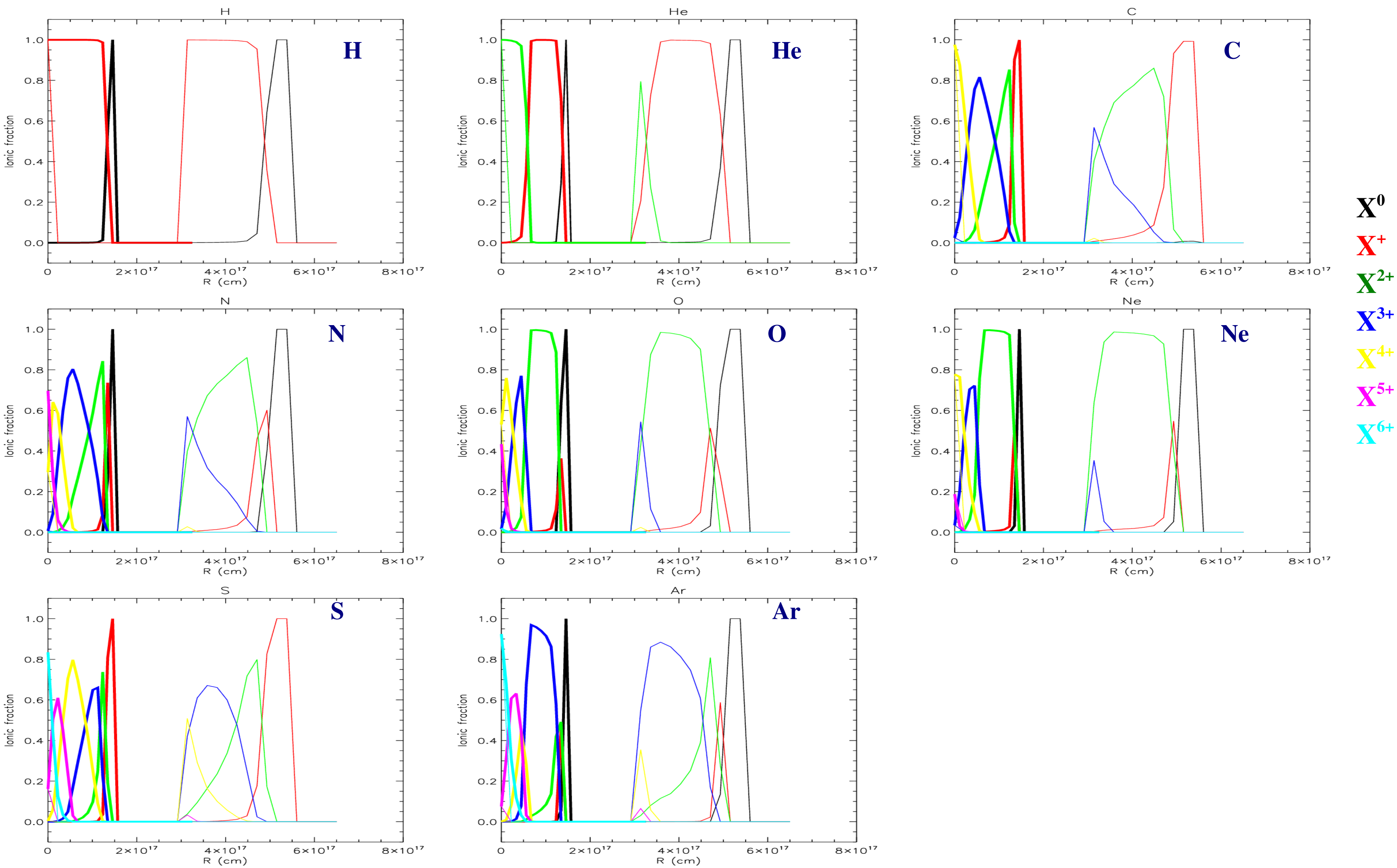

Results: the ionization structure changes with shape...

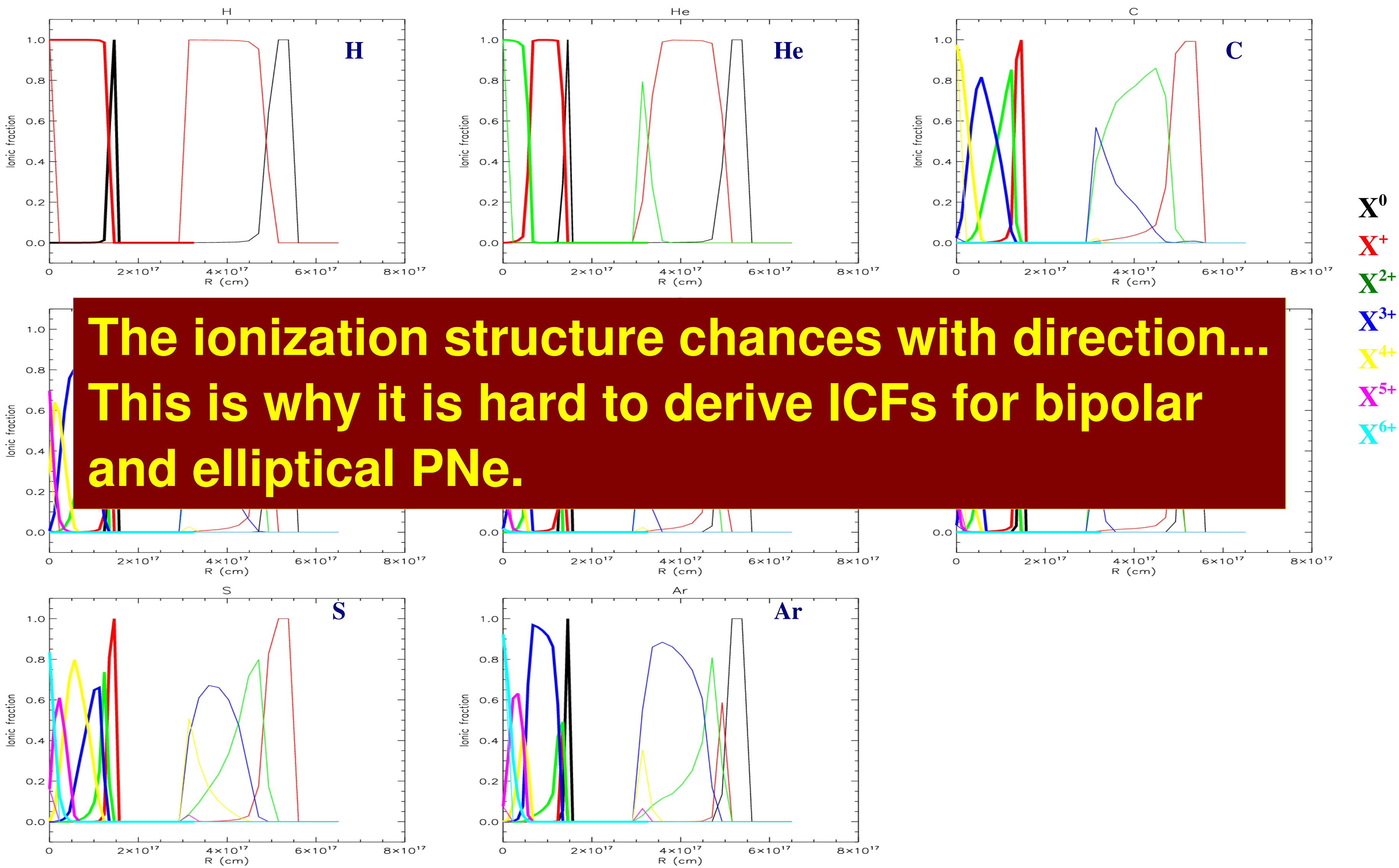

The ionization structure chances with direction... This is why it is hard to derive ICFs for bipolar and elliptical PNe.

Results: $KB94_{ICF}$ versus MOC_{ICF}

- Line intensities given by MOCASSIN for the **126 models** are used to obtain: He/H;
  ionic abundances of the various species;
  and **KB94's ICF**
- MOC ionic fractions return the true ionization correction factors, **MOC_{ICF}**

Results: $KB94_{ICF}$ versus MOC_{ICF}

- Line intensities given by MOCASSIN for the **126 models** are used to obtain: He/H; ionic abundances of the various species; and **KB94's ICF**
- MOC ionic fractions return the true ionization correction factors, $\mathbf{MOC_{ICF}}$

The $\mathbf{KB94_{ICF}/MOC_{ICF}}$ ratio will tell us which are the additional corrections we should apply to the KB94 scheme in order to derive more robust abundances for BIPOLARS and ELLIPTICALS!

(Gonçalves, Wesson, Morisset, Barlow & Ercolano., in prep.)

$KB94_{ICF}$ / MOC_{ICF} : NITROGEN

Optical + IR

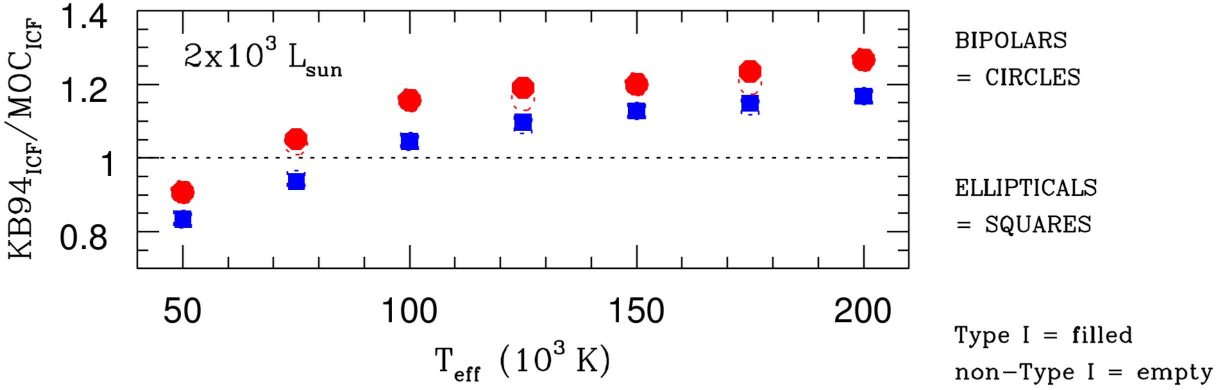

KB94$_{ICF}$ / MOC$_{ICF}$: NITROGEN

Optical + IR

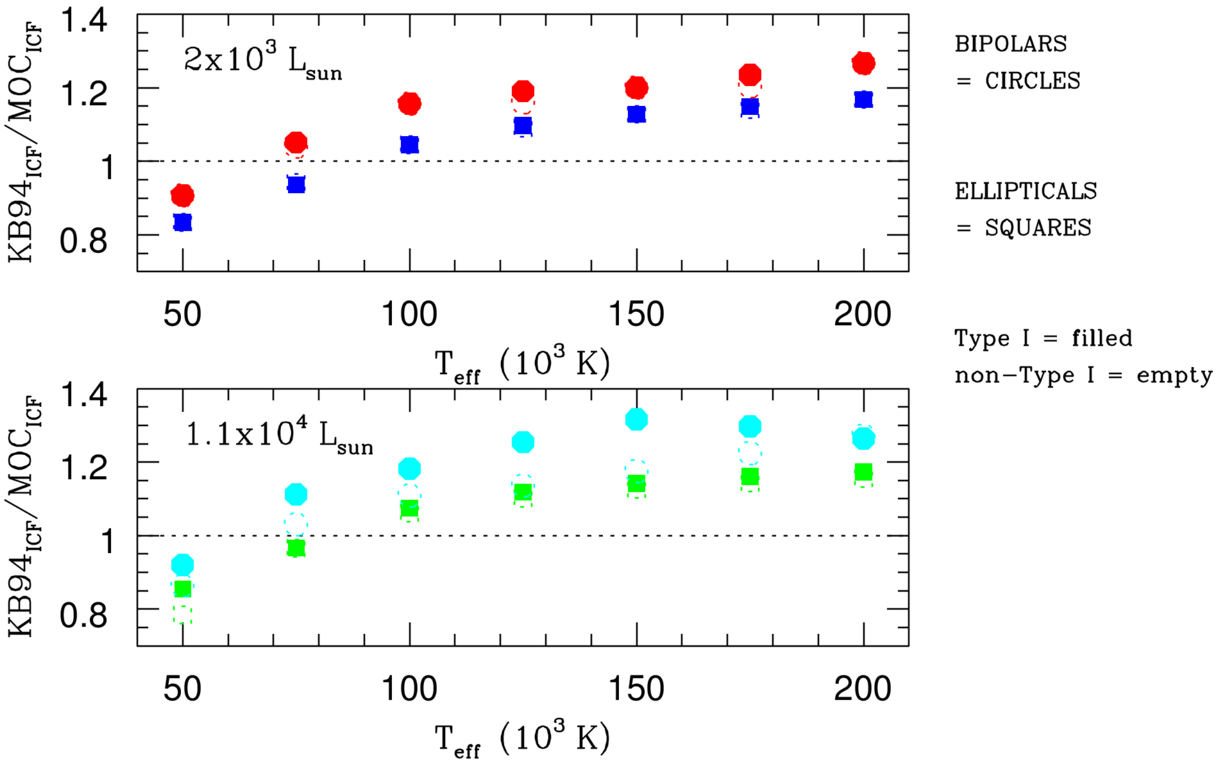

$KB94_{ICF}$ / MOC_{ICF} : NITROGEN

Optical + IR

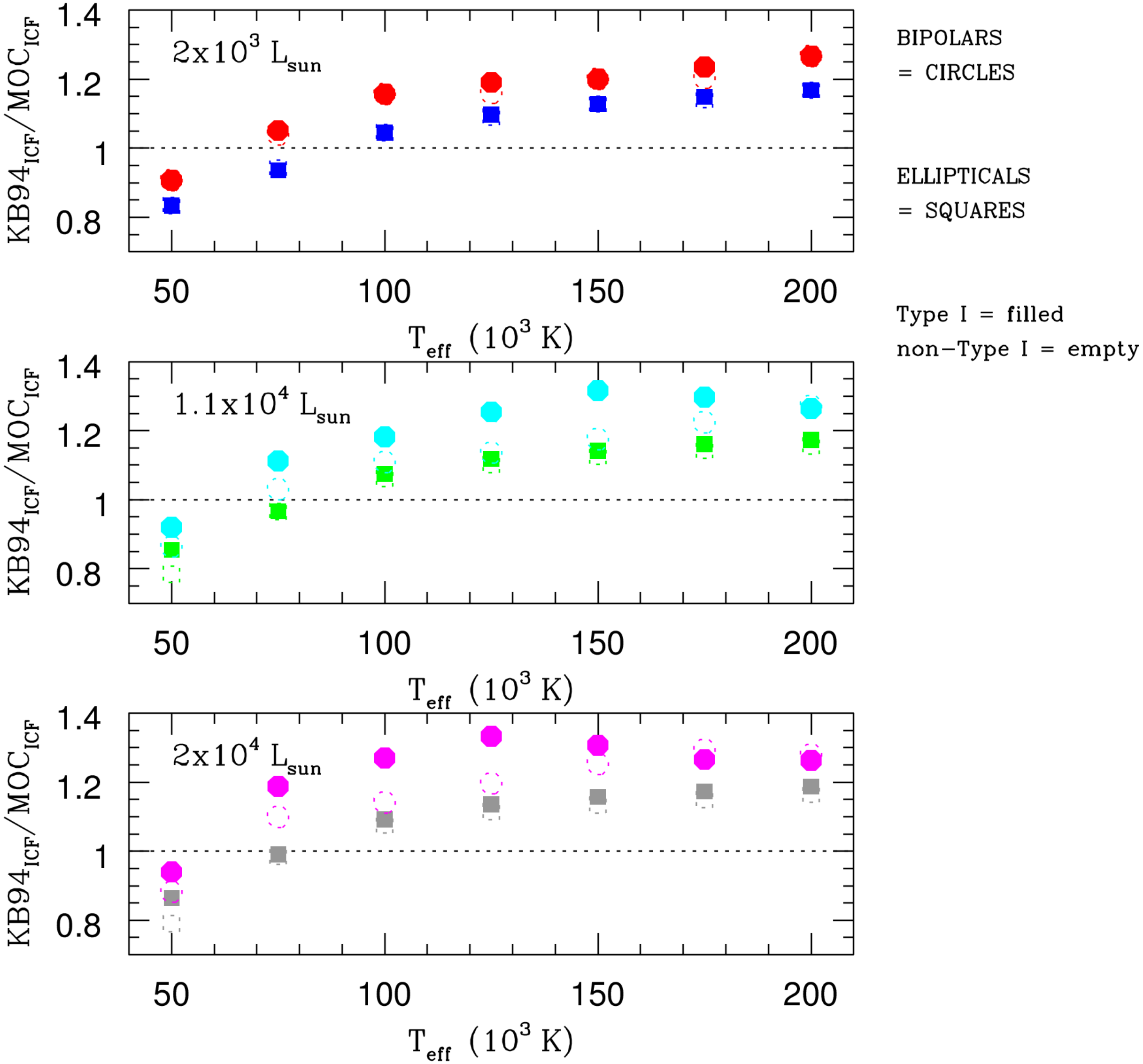

$KB94_{ICF}$ / MOC_{ICF} : NITROGEN

Optical + IR

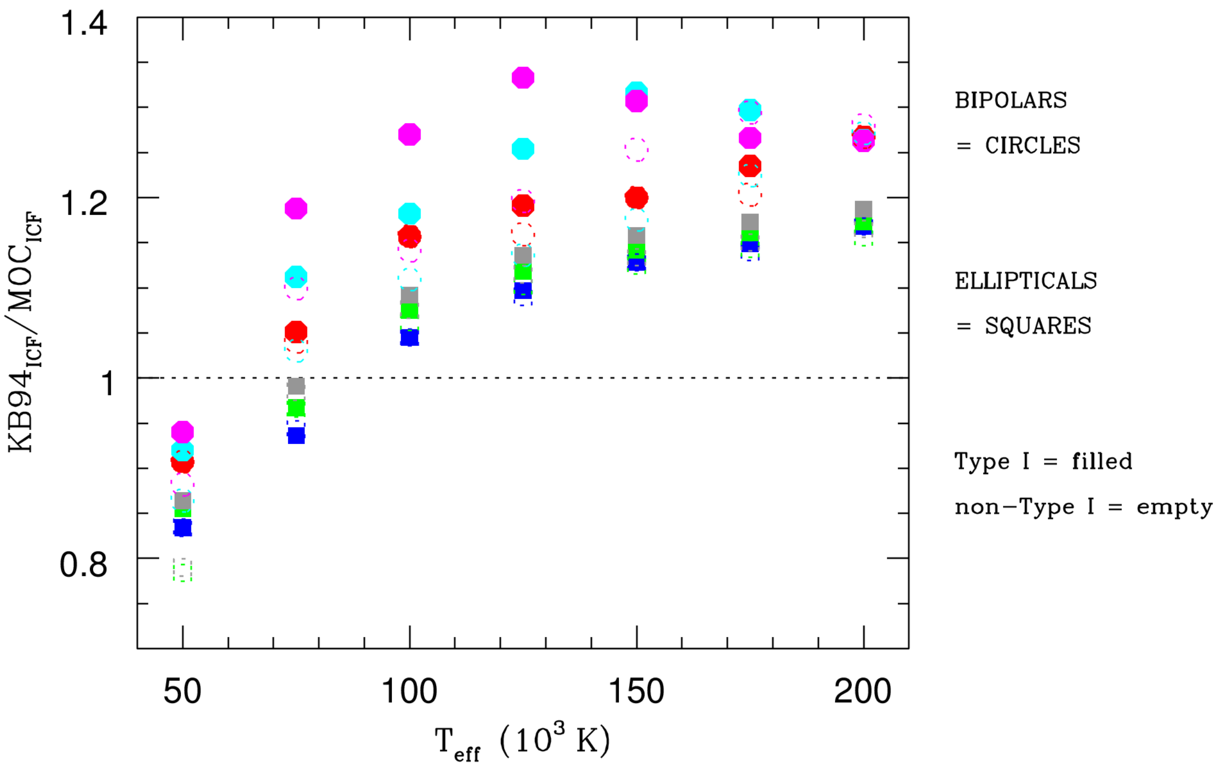

KB94$_{ICF}$ / MOC$_{ICF}$: OXYGEN

Optical + IR

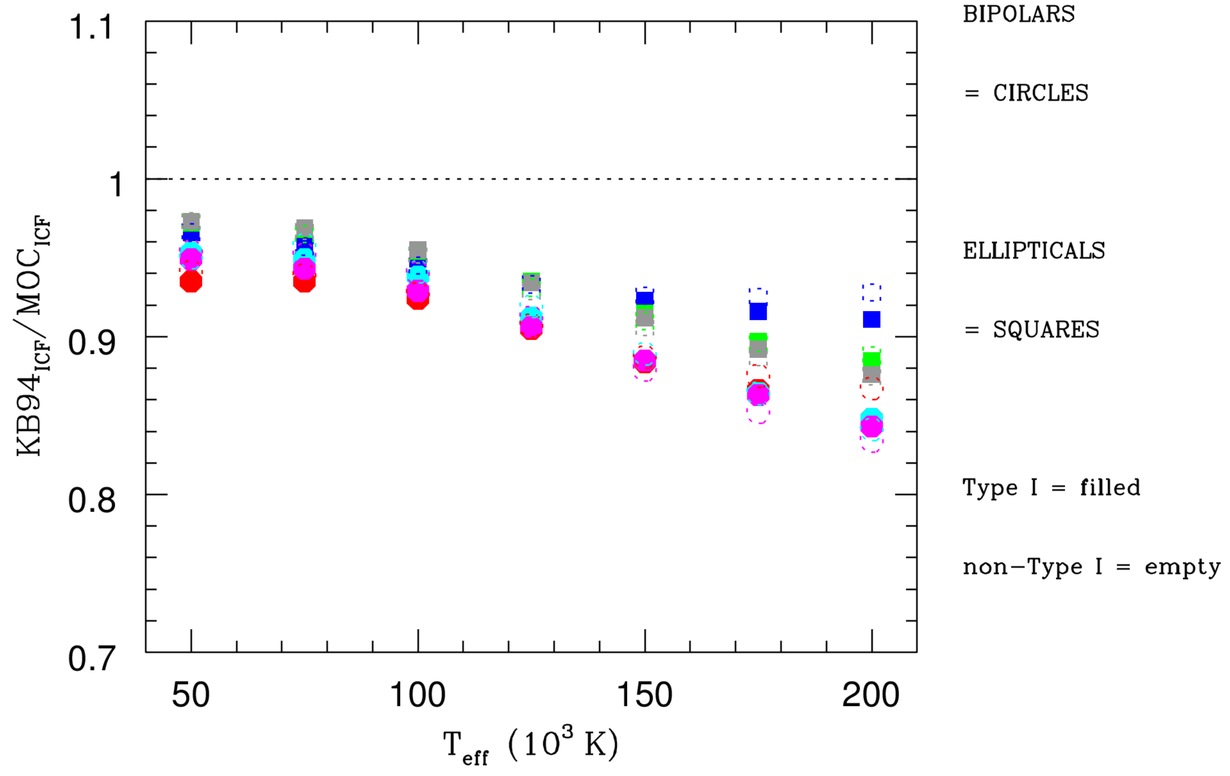

$KB94_{ICF}$ / MOC_{ICF} : NEON

Optical + IR

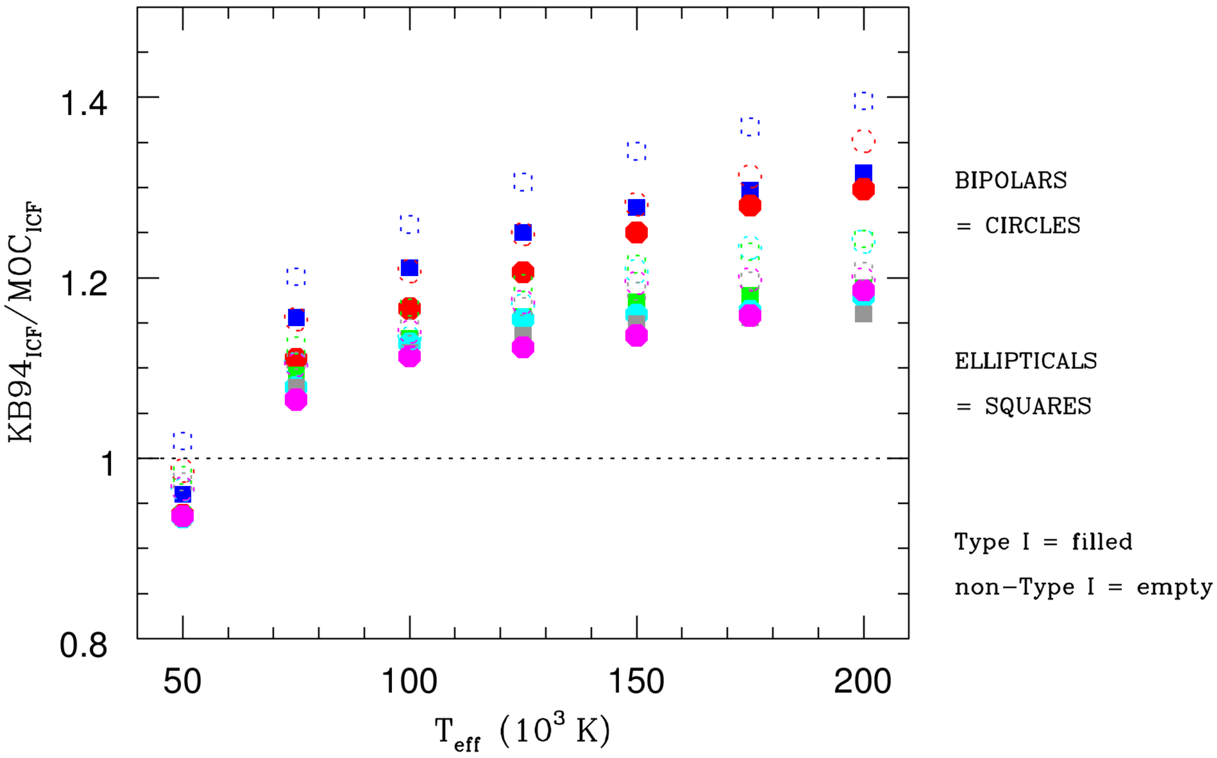

$KB94_{ICF}$ / MOC_{ICF} : SULPHUR

Optical + IR

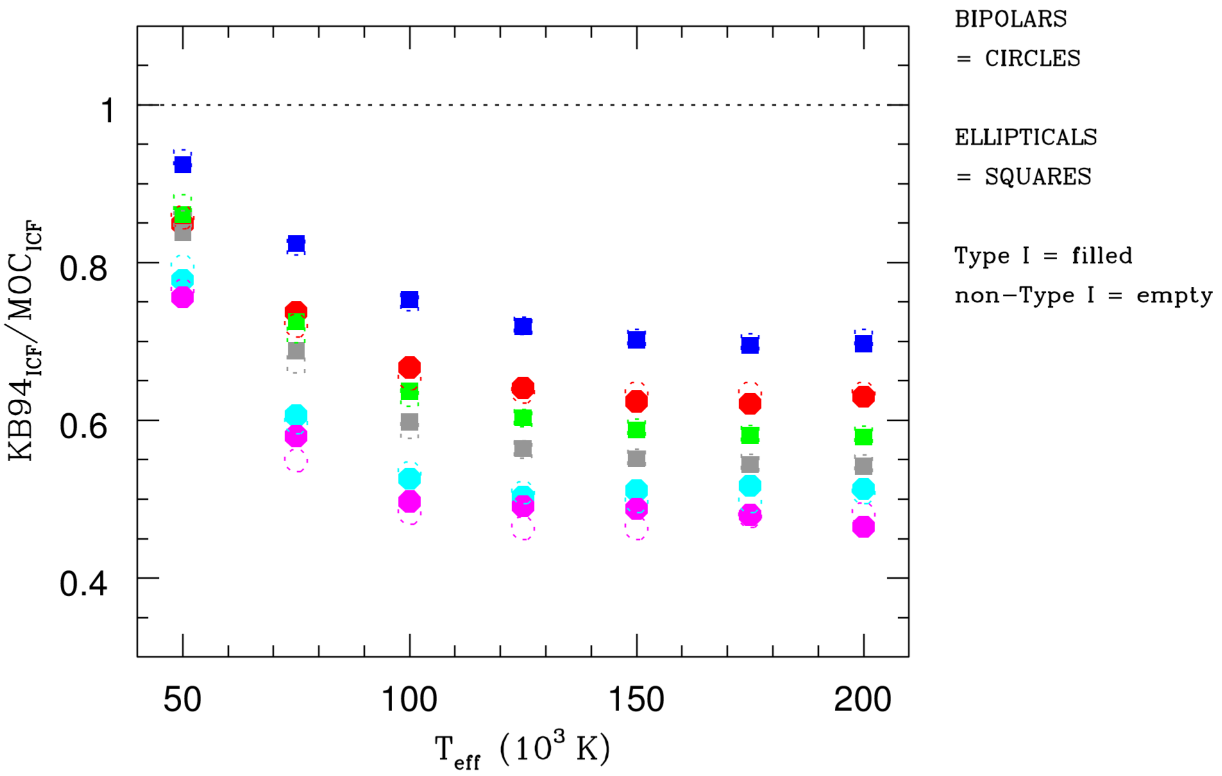

$KB94_{ICF}$ / MOC_{ICF} : ARGON

Optical + IR

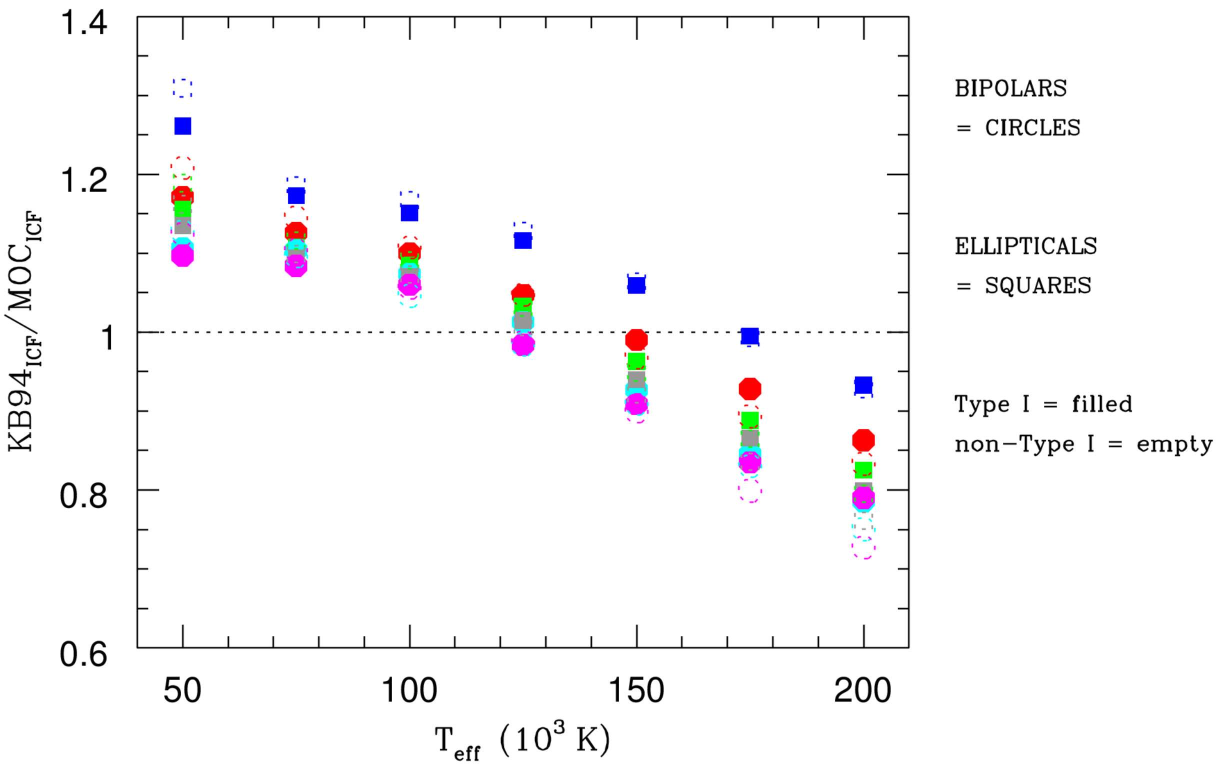

Results: $KB94_{ICF}$ versus MOC_{ICF}

Discrepancies in between ICF and true abundances

- Vary with T_{eff} as much as with shape, and they also change with luminosity and chemical type

- Are in general higher for bipolars than for ellipticals

- In the worst cases, they amount to B (E):

  up to **33 (19)%** for **N** (under & over estimated)
  up to **17 (13)%** for **O** (under)
  up to **40 (40)%** for **Ne** (over)
  up to **55 (50)%** for **S** (under)
  up to **28 (24)%** for **Ar** (under & over)

Results: KB94$_{ICF}$ versus MOC$_{ICF}$

Discrepancies in between ICF and true abundances

- Vary with T_{eff} as much as with shape, and they also change with luminosity and chemical type
- Are in general higher for bipolars than for ellipticals
- In the worst cases, they amount to B (E):

up to **33 (19)%** for **N** (under & over estimated)
up to **17 (13)%** for **O** (under)
up to **40 (40)%** for **Ne** (over)
up to **55 (50)%** for **S** (under)
up to **28 (24)%** for **Ar** (under & over)

What about if we include the UV spectrum in the analysis?

KB94$_{ICF}$ / MOC$_{ICF}$: NITROGEN

Optical + IR

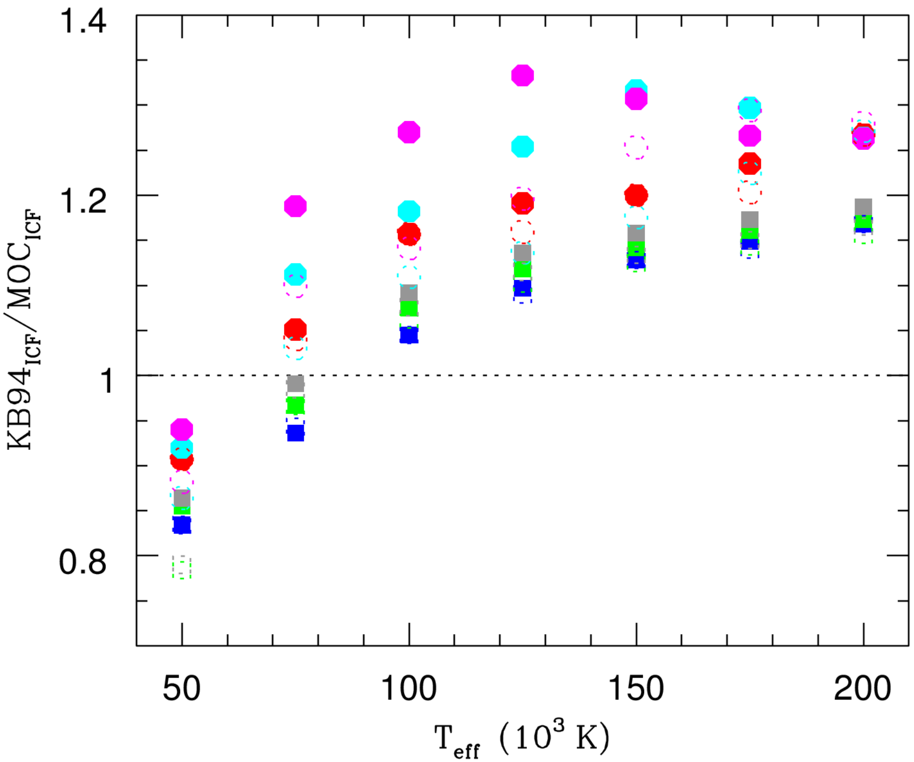

UV + Optical + IR

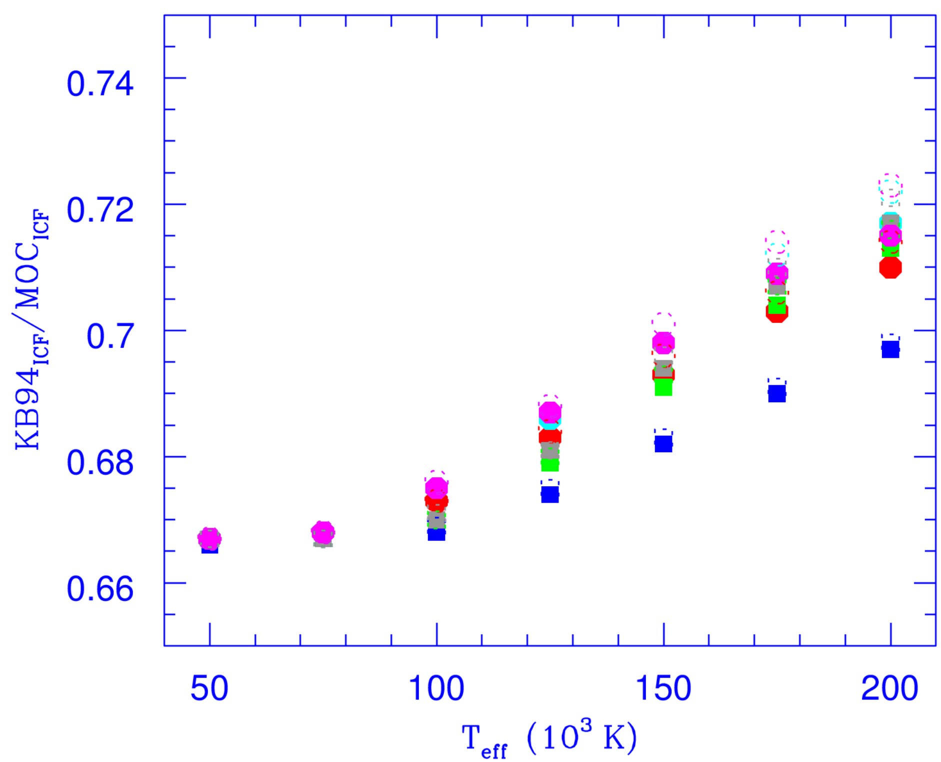

Missing ions: N^{2+}
N^{3+}

Missing ions: N^{2+}
(UV, but too faint)

$KB94_{ICF}$ / MOC_{ICF} : OXYGEN

Optical + IR

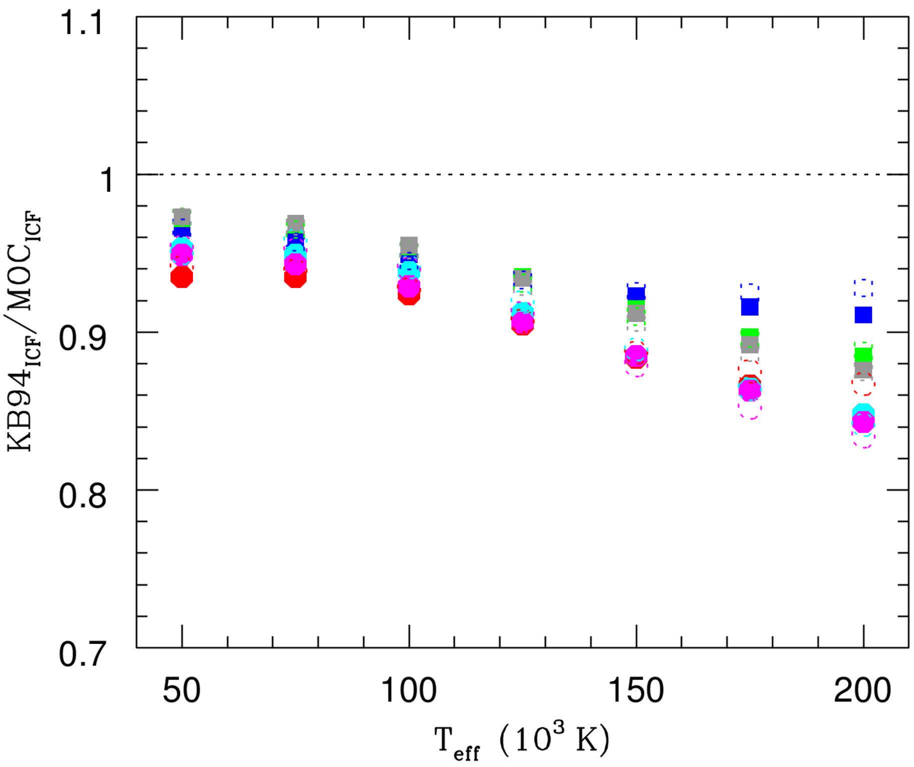

Missing ions: O^{3+}
O^{4+}

UV + Optical + IR

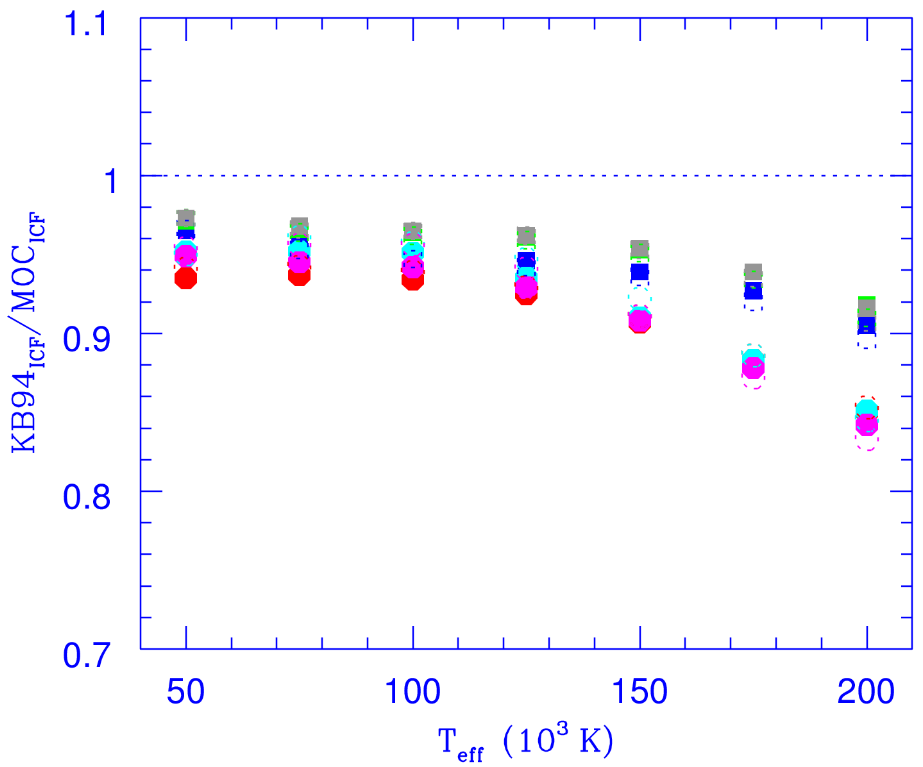

Missing ions: O^{4+}

$KB94_{ICF}$ / MOC_{ICF} : NEON

Optical + IR

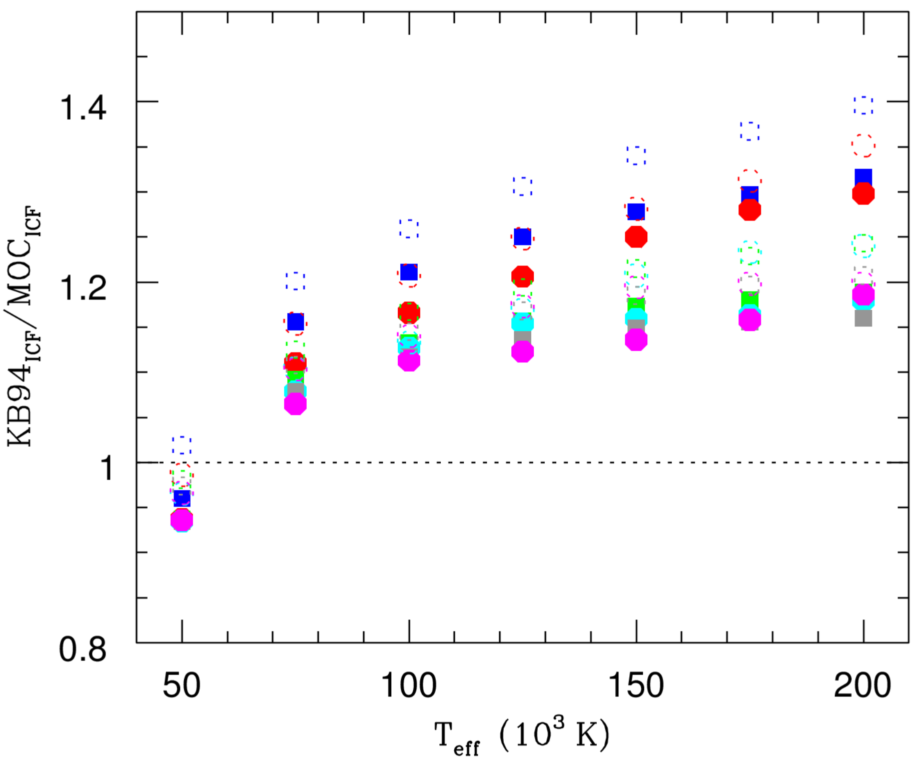

Missing ions: Ne^{3+}
Ne^{4+}

UV + Optical + IR

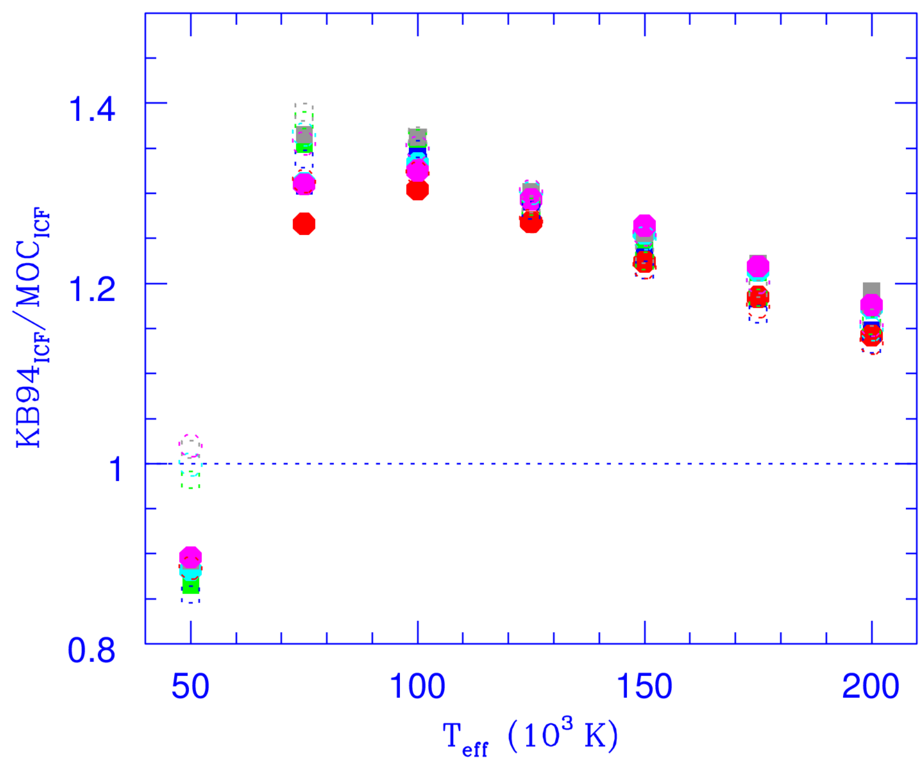

Missing ions: Ne^{3+}
(optical, but too faint)

In conclusion

To account for the different morphologies, the tools to derive empirical abundances need to be (and are being) improved (Gonçalves et al.; Delgado-Inglada et al.)

Discrepancies between ICF and true abundances

- **Vary with T_{eff} as much as with shape, and they also change with luminosity and chemical type**
- **Are in general higher for bipolars than for ellipticals**